# Streamlined Access to Substituted Benzothieno- S , S -Dioxide-Benzofuran (BTOBF): Properties and Application in Solution-Processed Organic Light-Emitting Diodes

Khaled Youssef, Akpeko Gasonoo, Magali Allain, Hayley Melville, Lionel Sanguinet, Gregory C Welch, Frédéric Gohier

# Streamlined access to substituted Benzothieno-*S,S*-dioxide-benzofuran (BTOBF): properties and application in Solution Processed Organic Light-Emitting Diodes

Khaled Youssef,[a] Akpeko Gasonoo,[b] Magali Allain,[a] Hayley Melville,[a] Lionel Sanguinet,[a] Gregory C. Welch,[b] Frédéric Gohier[a*]

[a] Univ Angers, CNRS, MOLTECH-ANJOU, SFR MATRIX, F-49000 Angers, France

[b] Department of Chemistry, University of Calgary, 2500 University Drive N.W., Calgary, Alberta T2N 1N4, Canada

**ABSTRACT:** Utilizing a streamlined five-step synthesis process, we have successfully produced a diverse set of adjustable benzo[4,5]thieno-S,S-dioxide-[3,2-b]benzofurans-based compounds through Michael's addition-elimination reaction, Suzuki-Miyaura coupling, and intramolecular oxidative C-H/C-H coupling, in 70-90% yields. The synthetic strategy employed demonstrates that the compounds can be modified on either side by introducing various types of groups at positions 2 and 3, with the possibility of extending the aromatic portion in place of the benzofuran. Thus, these compounds exhibit a distinctive dual-state emission, showcasing very good quantum yields up to 63% in solid state and 83% in solution. Additionally, these compounds have been integrated into ambient condition, solution-processed, non-doped OLEDs, demonstrating promising results with a luminance of 850 cd/m$^2$ and a turn-on voltage of 3.50 V.

**KEYWORDS**: benzothieno-S,S-dioxide-benzofurane, solution processed OLED, oxidative C–H/C–H coupling

# 1-Introduction

In recent years, organic light-emitting diodes (OLEDs) have emerged as key technology, attracting attention for their efficiency, vibrant colors, and diverse applications in daily life. A substantial effort has been devoted to enhancing OLED technology, addressing luminance efficiency, color range, device stability, and fabrication techniques.[1-3] Evaporation is the technique most commonly used to prepare these OLEDs, but it is also possible to deposit them in solution and thus print them. The review by Han et al[4] in 2023 indicates the state of the art in this field. Solution deposition is very often limited to the active layer but already raises questions about the orthogonality of the solvents used to avoid any redissolution of the layer on which deposition is taking place. OLEDs are complex devices made up of many layers, each with an important role to fulfill. Printing all the layers therefore becomes a real challenge. Very few publications mention OLEDs prepared entirely by solution processing.[5, 6] The central layer, the one that emits, must undoubtedly be regarded as the crucial component of OLEDs. Within the field of organic emitters, sulfones are widely used. [7, 8] Among sulfones, cyclic sulfones such as benzothiophene S,S-dioxide (BTO) have the advantage of greater delocalization, especially when fused with fluorenes or carbazoles. These long-extended systems are highly emissive and are applied in OLEDs.[9, 10] BTOs can also be combined with benzofurans which is less common. This system known as Benzo[4,5]thieno-S,S-dioxide-[3,2-b]benzofuran (BTOBF), has emission properties that merit attention. Indeed, Li et al. have shown that by substituting the BTOBF with a N,N-diphenylaniline (TPA) in position 2, for example, luminance can reach over 12,000 cd/m$^2$ with a turn-on voltage of around 3 V.[11] A patent also mentions the insertion of aromatic nitrogen derivatives in position 2 and/or 8, leading to high luminous efficacy and very high stability.[12] The main access route is via the oxidation of benzo[4,5]thieno[3,2-b]benzofuran (BTBF) using mCPBA[12, 13] or urea–hydrogen peroxide.[14] BTBF is more popular because it is easier to access and therefore more studied. It shows high fluorescence quantum yields, and favorable charge carrier mobilities.[15, 16] Various approaches to BTBF are documented in the literature (Scheme 1). Zhu et al. [17] described an

Ullman-type intramolecular C-O reaction from 3-bromobenzothiopene derivative to access BTBF. Li et al.[18] used the same route but doing in one pot intermolecular Suzuki coupling and subsequent intramolecular Ullmann C–O coupling reactions. In the same vein, Li group employed intramolecular dehydrogenative C–H/O–H coupling.[19] Kuninobu et al.[20] and Miura group[21] demonstrated Pd-catalyzed intramolecular oxidative C–H/C–H coupling, and Mitsudo et al[22] reported an electro-chemical synthesis via dehydrogenative C–H/S–H coupling. John group[23] presented a metal-free synthetic route through the annulation of 3-nitro benzothiophene with phenols. The BTBF core can also be obtained by flash pyrolysis of 2-methoxyphenyl and 2-methylthiophenyl phosphorus ylide, but it becomes complicated to functionalize the structure upstream of this step.[24] Substitution of the BTOBF core will therefore depend on the substitution pattern of BTBF, and it may prove somewhat time-consuming in terms of synthesis and challenging to access certain positions of BTBF. BTBF oxidation is not the sole pathway to BTOBF, as it is also possible to directly cyclize BTO into BTOBF via dehydrogenative C-O coupling with copper, as demonstrated by Suga group. [25] However, only one example has been described.

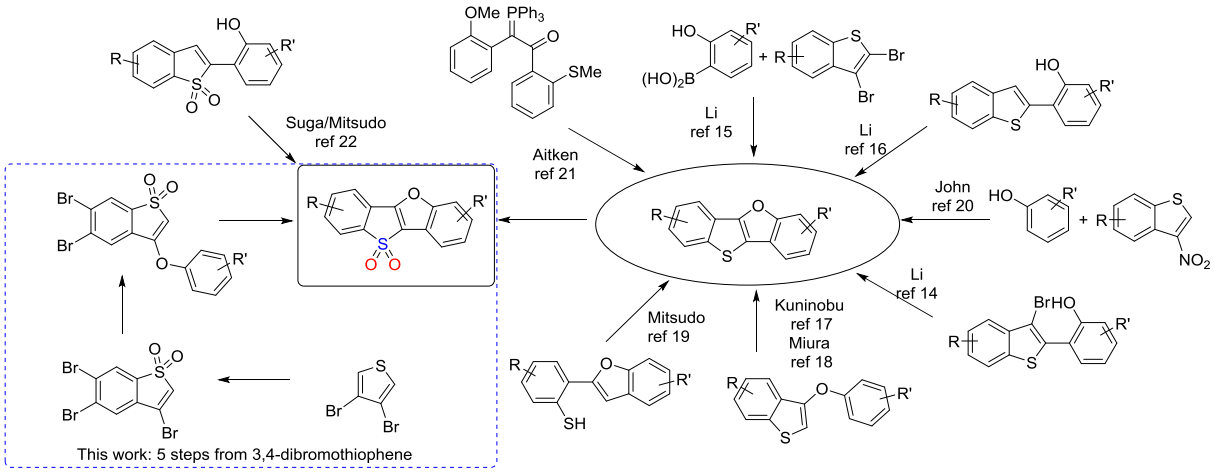


**Scheme 1**. Various access to BTBF and BTOBF

Here we present a novel 5-step approach to access BTOBF starting from a basic brick, such as 3,4-dibromothiophene. Notable advancements include the ability to introduce various groups at positions 2 and 3 of the BTOBF through Suzuki coupling, as well as expanding the aromatic framework by incorporating aromatic alcohols via the Michael reaction on the BTO. We also present the optoelectronic properties and the effects of various modifications on these properties. Since the compounds exhibit high emissivity, as all members of this family, OLED devices have also been fabricated, prioritizing solution-based deposition over evaporation. This approach allows for the potential to fully print the OLEDs at a later stage.

# 2-Results and discussion

Compound **1** has been produced from 3,4-dibromothiophene according to our previous published procedure.[26] The latter is oxidized and then heated in acetic acid. Dimerization is then observed, followed by $SO_2$ extrusion and elimination of a bromine atom. Oxidized benzothiophene displays a particular reactivity, since the thiophene moiety is no longer aromatic and the sulfone is conjugated to the double bond, making it an excellent Michael acceptor. Addition of phenol, 1-naphthol, 6-bromo-2-naphthol, and 1-pyrenol as nucleophiles in the presence of potassium carbonate in DMF at 70°C overnight leads to adducts 1-4, followed by in situ elimination of bromine to reform the conjugated system. Compounds **2a,d-f** were formed with yield up to 80%. After purification by column

chromatography, **2a** was subjected to Suzuki-Miyaura coupling reaction with (4-(trifluoromethyl) phenyl) boronic acid and (4-fluorophenyl) boronic acid and **2a,d-f** were reacted with (4-(diphenylamino) phenyl) boronic acid. **3a-f** were obtained with yields up to 98%, the reaction yields not being sensitive to the electrowithdrawing or electrodonating character of the boronic acid derivatives. Finally, Pd-catalyzed intramolecular oxidative C–H/C–H coupling has been realized on **3a-f** to afford benzo[4,5]thieno-S,S-dioxide-[3,2-b]benzofuran derivatives **4a-f** (see Scheme 2). This procedure has never been carried out in the presence of sulfone and leads to good yields. This step cannot be carried out if the bromines of the benzene ring are still present. A few attempts were made from **2a** to afford a complex mixture of compounds. The expected compound **4g** was obtained in very small quantities. All compounds have been fully characterized and verified by $^{1}H$ and $^{13}C$ NMR spectroscopy and HR mass spectrometry (see ESI).

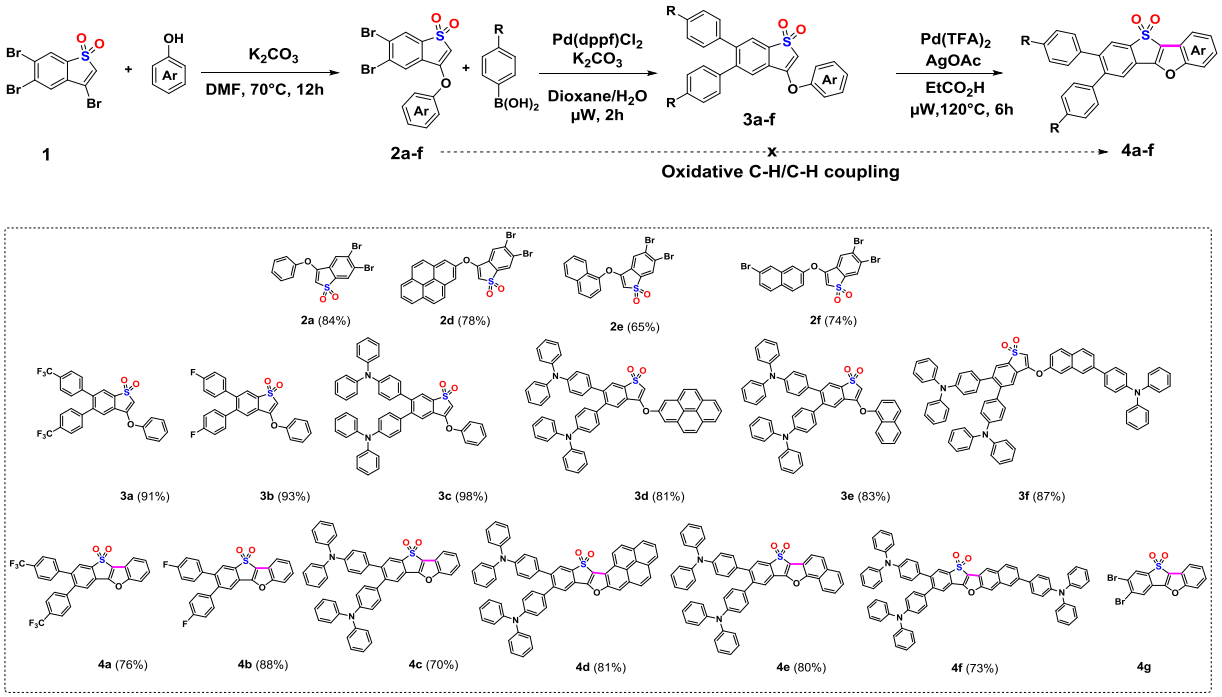


**Scheme 2**. Synthetic route of BTOBFs and their derivatives

## Optical properties

The UV-visible optical absorption and fluorescence properties were measured in dichloromethane (DCM) solutions (Figure 1a). The photophysical and electronic characteristics of these compounds are summarized in Table 1. The various BTOBFs show optical absorbance spectra with fine structuring, in line with what is described in the literature. Indeed, absorbance spectra of unoxidized benzothienobenzofuran[18] have been described with fine structuring due to π-π* transitions, and another paper on BTOBFs substituted by either halogens or an electron donor (TPA or N-phenylcarbazole)[11] implies an internal charge transfer due to the sulfone.

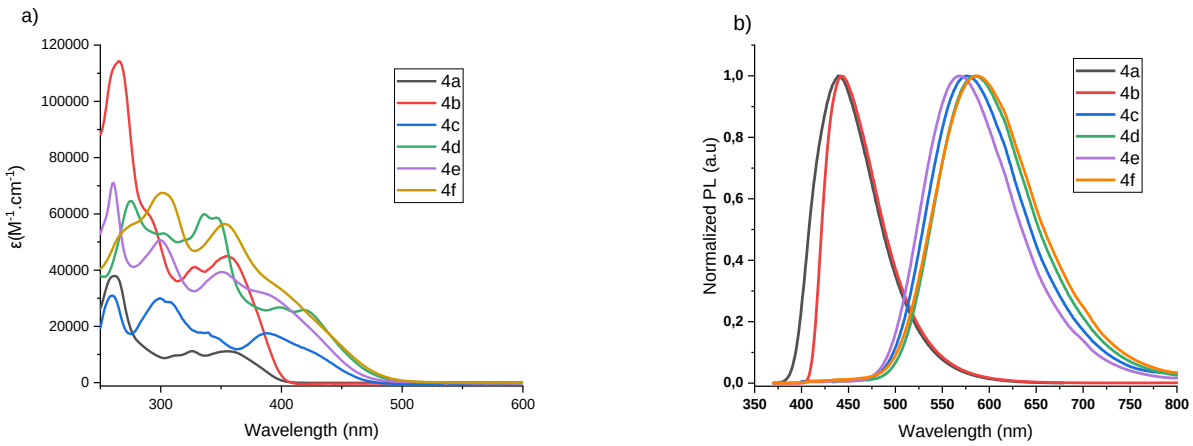


**Figure 1**. (a) UV-Vis absorption spectra of **4a-f** in DCM (10-5 mol/L); (b) Fluorescence spectra of **4a-f** in DCM ($10^{-6}$ mol/L)

Looking at the optical absorption spectra, we can see that the substituents play an active role in the optical absorbance. Indeed, compounds **4a** and **4b** bearing $CF_3$ or F were found to absorb in the UV region with some maxima absorption of 260/326/358 nm and 265/326/355 nm, respectively, and with an onset absorption of 410 and 412, respectively, whereas BTOBFs with TPAs show a red shift in absorption due to the electron donor effect and significant conjugation. Switching from benzofuran **4c** to naphthofuran **4e** has little effect on optical absorbance, and using pyrenofuran **4d** results in a red shift of around 15 nm. Ma[18] showed on BTBF that extension with naphthalene shifted the spectrum 35 nm towards the red. In our case, adding naphthofuran to the BTOBF bearing two TPAs (compound **4c** versus **4e**) does not shift the optical absorption towards longer wavelengths. Emission spectra, also carried out in DCM with concentrations of 10^-6 M, show very significant Stokes shifts. These were determined by the difference between the emission and absorption maxima (last band on the spectrum for absorption). Thus, **4a** and **4b** that emit in the blue region at 439 nm and 442 nm, respectively have a Stokes shift of 0.72 and 0.68 eV nm whereas **4c**, **4d**, **4e** and **4f** present even higher stokes shifts with 1.03, 0.84, 1.03 and 1.40 eV respectively. Their maximal emissions have been measured in between 575 and 587 nm. The concentrations of the different solutions were then halved to check for the possible presence of excimer, but emission spectra remain unshifted. Thus, it is conceivable that this shift between absorption and emission must be due to a stabilization of the molecule in the excited state with either a modification of the geometry and/or relaxation of the excited state solvent.[27, 28] The fluorescence quantum yields (Φf), done by using integration sphere measurements, for **4a-4f** in dichloromethane are determined as 80, 73, 83, 72, 76, 46, and 38, 36, 63, 12, 19, 24 in solid state respectively. Overall, emission in solution is more efficient than in the solid state, maybe due to aggregation. It has been shown with carbazole-2-substituted BTOBF[12] that quantum yields in the solid state cane be doubled to almost unity when used as a dopant, thus limiting their aggregation.

Crystals of **2a**, **4a**, **4b**, **4c**, **4d** and **4g** were obtained to study the effect of changes on structure (see SI). Thus, the structure of compound **2a** shows a phenyl group in a plane, forming a dihedral angle of 119° with the plane in which the benzothiophene lies, which is quite normal (Figure 2). Cyclization must lead to a completely planar system, and this is the case for compound **4g** and compound **4b**. On the other hand, when slightly larger groups such as TPA or Ph-$CF_3$ substitute benzothienobenzofuran, the system curves by 12° (**4c**) and 11° (**4a**) respectively. When the benzofuran moiety is extended with pyrene, the system deforms a little further, with a pyrene-induced torsion (see Figure 2).

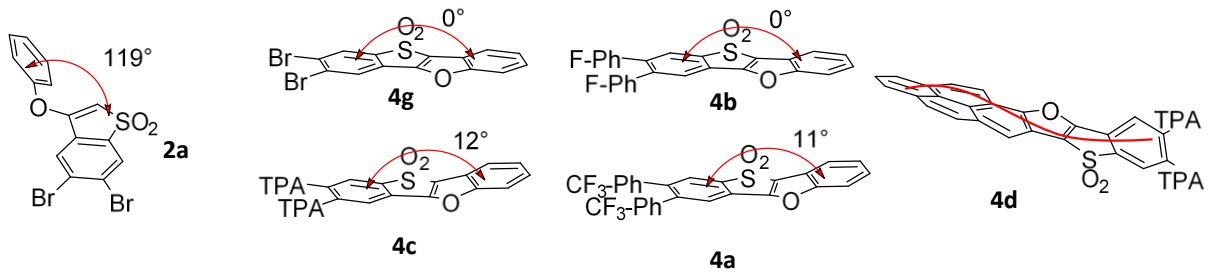


**Figure 2.** Representation of the BTOBF geometry depending on substitution.

Examining the organization within the crystals, regardless of the substitution, the molecules systematically arrange head-to-tail in pairs with a pi-stacking interaction between the benzothienobenzofurans. Substitutions at the ends of the molecules cause deformation if the packing is slightly larger. Looking at the crystal lattice stacking, the organization is very complex for compound **4c**, which nevertheless shows greater emission than all the other compounds both in solid and solution. The BTOBF cores of **4c** are paired in perfectly parallel planes, but within the crystal lattice several orientations are observed. Note that the distance between these planes (3.80 Å) is greater than in other crystals of the same family (3.70, 3.56 and 3.50 Å for **4a**, **4b** and **4d** respectively). For compounds **4a**, **4b** and **4d**, the organization is more obvious. For **4d**, as with **4a**, all BTOBF cores are in parallel planes uniformly oriented within the lattice, whereas for **4b**, the organization is different but remains clearly illustrated as shown in Figure 3. It is therefore plausible to imagine that, in the solid state, poor organization will be more favorable for emission than compounds showing high organization.

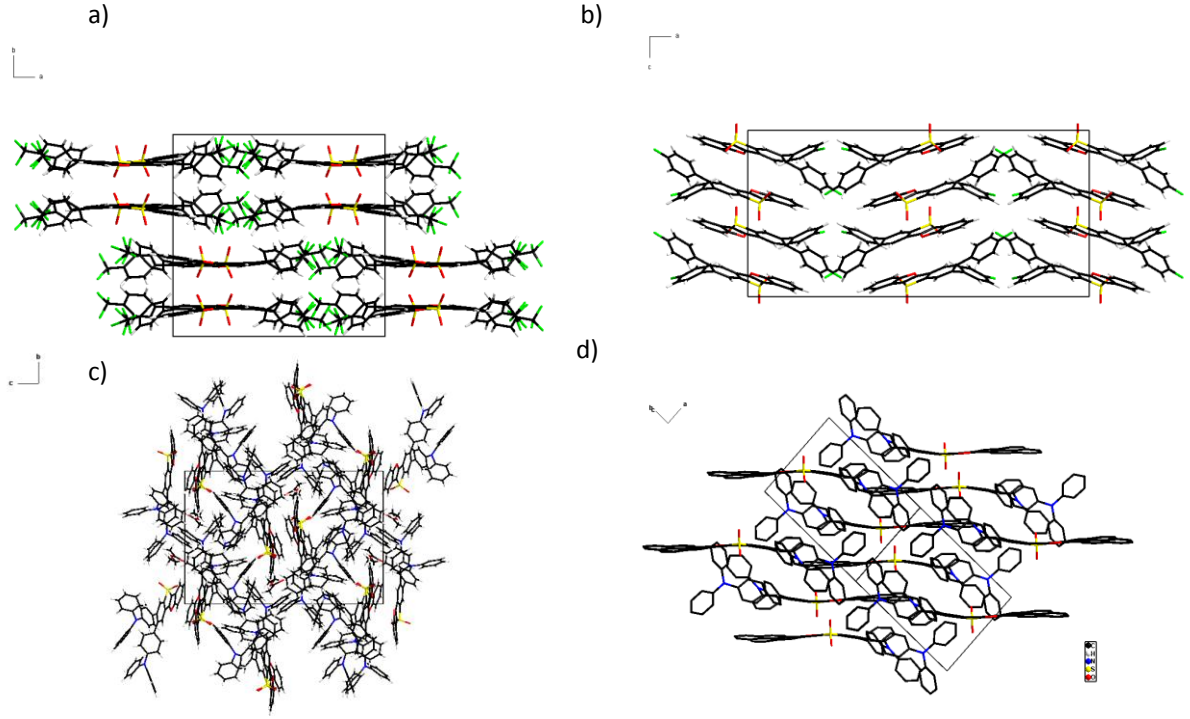


**Figure 3**. Packing structures of a) **4a**; b) **4b**; c) **4c**; d) **4d**.

Photoelectron spectroscopy in air (PESA) measurements were subsequently performed and HOMO energy levels of −5.62, -5.63, -5.60, and −5.60 eV were calculated for **3c-f,** respectively. We could not measure the highest occupied molecular orbital (HOMO) energy levels of **4a-b** as it's out of instrument boundaries and thus they should probably be lower due to the presence of electrowithdrawing groups (F and $CF_3$). Once cross-tabulated with UV-visible experiments, the

corresponding lowest unoccupied molecular orbital (LUMO) energy levels -3.10, -3.15, -3.00, and -3.16 eV were calculated by adding the energy determined from the optical band gap (thin-film spectra).

**Table 1**. Photophysical, and electrochemical properties of **3a-f**

| | $\lambda_{abs,max}$ [a] (nm) | ε ($M^{-1}.cm^{-1}$) | $\lambda_{onset}$ [b] (nm) | $\lambda_{PL,max}$ in DCM[c] (nm) | $\lambda_{PL,max}$ solid[d] (nm) | *Φ(%)* | | HOMO[g] (eV) | LUMO[h] (eV) | $E_g^{opt}$[i] (eV) |
|---|---|---|---|---|---|---|---|---|---|---|
| | | | | | | *powder*[e] | *solution*[f] | | | |
| **4a** | 262 | 38000 | 410 | 439 | 447 | 38 | 80 | | | 3.03 |
| **4b** | 265 | 114000 | 412 | 442 | 471 | 36 | 73 | | | 3.01 |
| **4c** | 260 | 31000 | 492 | 575 | 536 | 63 | 83 | -5.62 | -3.10 | 2.52 |
| **4d** | 275 | 64000 | 500 | 586 | 535 | 12 | 72 | -5.63 | -3.15 | 2.48 |
| **4e** | 261 | 71000 | 492 | 569 | 540 | 19 | 76 | -5.60 | -3.10 | 2.52 |
| **4f** | 302 | 67000 | 509 | 587 | 436 | 24 | 46 | -5.60 | -3.16 | 2.44 |

[a] Maximum absorption in DCM. [b] $\lambda_{onset}$ absorbance on thin films. [c] Measurement done on $10^{\Lambda-6}$ M solution in DCM. [d] Measurement done on powder.[e] Absolute fluorescence quantum yield in powder measured by integration sphere instrument.[f] Absolute fluorescence quantum yield in DCM measured by integration sphere instrument. [g] Determined by photoelectron spectroscopy in air (PESA). [h] LUMO = HOMO + $E_g^{opt}$. [i] Estimated from the low-energy absorption onset of thin films.

## Electrochemical properties

Electrochemical properties were measured using cyclic voltammetry (CV) with ferrocene/ferrocenium as the reference. All CV curves are depicted in Figure 4, and the corresponding data are compiled in Table 2.

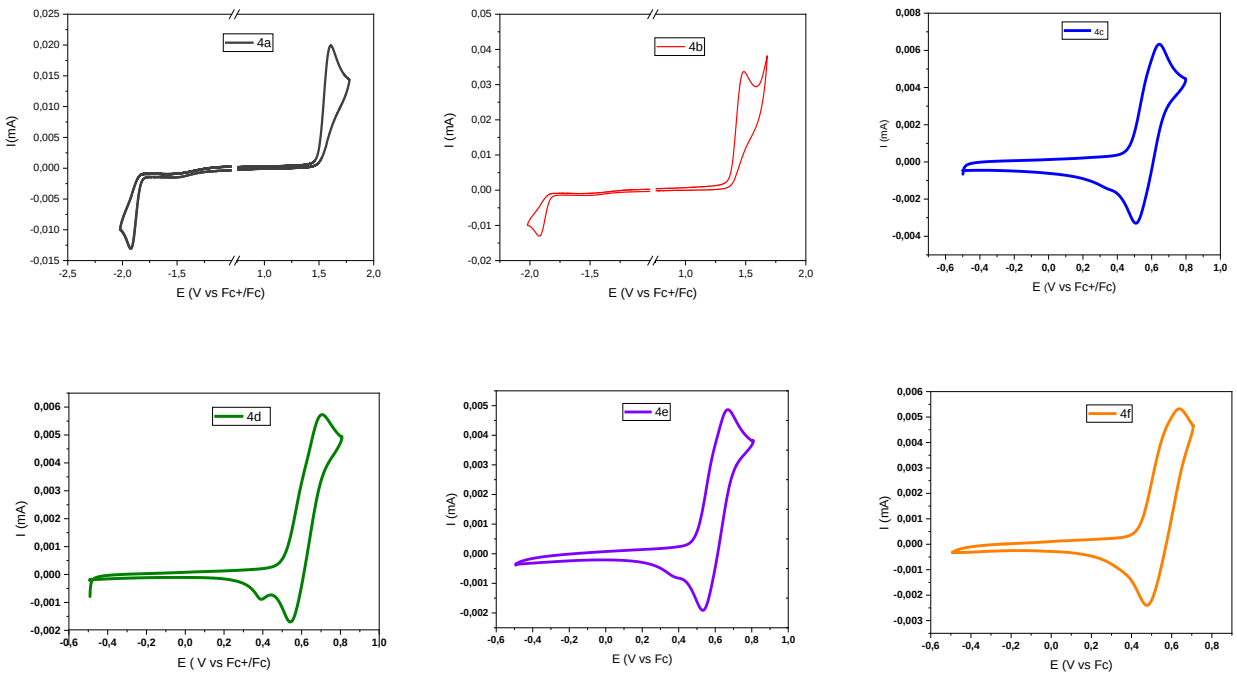


**Figure 4.** Cyclic voltammetry of compounds **4a-b** (C = $10^{-3}$ mol/L, $CH_3CN$) and **4c-f** (C = $0.5x10^{-3}$ mol/L DCM) in 0.1M $Bu_4NPF_6$/solvent, scan rate 100 mv/s.

The substitution of the BTOBF core leads to two different voltammetric profiles. The one with halogens (**4a** and **4b**), which are electronically withdrawing, shows one irreversible oxidation, which is expected as the radical cation doesn't seem to be sufficiently stabilized. On the other hand, one irreversible reduction wave is also visible due to the stabilization of the LUMO energy level. The addition of TPA results in a system that becomes quasi-reversible but no longer allows the observation

of reduction in the solvent's study window. Thus, **4c-f** exhibit very similar voltammograms, with a visible shoulder on the voltammograms of **4c-e** upon return. This is most likely due to TPA dimerization,[29] which deposits on the electrode, forming a new system that is reduced when the potential returns to 0. **4a-b** are much more difficult to oxidize, leading to HOMO energy levels lower than -6.00 eV (-6.30 eV and -6.18 eV), whereas for **4c-f**, the levels range from -5.24 eV to -5.30 eV. The number of TPA substituents on BTOBF does not seem to have an effect on these levels.

**Table 2**. Electrochemical data of compounds **4a-f**

| Compound | $E_{ox}/E_{red}$ (V)[a] | HOMO/LUMO [b] (eV) |
|---|---|---|
| **4a** | 1.50/-1.82 | -6.30/-2.98 |
| **4b** | 1.38/-1.83 | -6.18/-2.97 |
| **4c** | 0.48 | -5.28 |
| **4d** | 0.50 | -5.30 |
| **4e** | 0.49 | -5.29 |
| **4f** | 0.44 | -5.24 |

[a] The values correspond to the onset of the oxidation or reduction wave. [b]Calculated from the empirical formula HOMO =-(4.8+$E_{ox}$) eV and LUMO = - (4.8-$E_{red}$) eV with $V/_{Fc+/Fc}$

## Device fabrication and Electroluminescent (EL) properties

Traditionally, for optimal performance, OLEDs are made up of an anode, a hole injection layer (HIL), a hole transport layer (HTL), an emissive layer (EML), an electron transport layer (ETL) and a cathode. The fabrication of solution-processed OLED devices has the advantage of being able to be manufactured on large surfaces, but requires the use of a solution that does not redissolve the layer to which it is applied. In this context, we need to determine compatibility of each layer with all the solvents considered. Previous work has enabled the homogeneous deposition of poly(3,4-ethylenedioxythiophene) and polystyrene sulfonate (PEDOT-PSS) (HIL) in water, onto which Poly(N-vinyl carbazole) (PVK as HTL) can be deposited in dioxane by spin coating or slot-die coating.[30] The various compounds were then dissolved at 30 mg/L in either ethyl acetate (AcOEt) or *o*-xylene. AcOEt has been identified as a solvent that does not solubilize PVK, however as depicted in Table 3, most of the molecules are insoluble in it. Solubility tests in *o*-xylene proved significantly better except for **4f**. Therefore, a solvent resistance test of PVK to *o*-xylene was conducted. Thin films of PVK were spin-coated onto pristine glass substrates from 10 mg/mL solutions in 1,4-dioxane. UV spectrum is then taken on the freshly deposited films and compared with spectrum of film exposed to *o*-xylene by spin-coating, simulating the deposition of a new layer. It shows 56% resistance to redissolution. Furthermore, the utilization of high molecular weight PVK (average molecular weight = 1100000 g/mol) increases its resistance to 93% (refer to the Supplementary Information). Since **4f** and **4d** were not soluble in *o*-xylene, *o*-dichlorobenzene was used to dissolve them. However, a major drawback of this solvent is that PVK is completely soluble in it, which means that **4f** could be deposited, but not on top of PVK.

**Table 3.** Solubility of **4a–f** and PVK in different organic solvents in C = 30mg/ml.

| Molecule | 4a | 4b | 4c | 4d | 4e | 4f | PVK |
|---|---|---|---|---|---|---|---|
| EtOAc | Yes | No | No | No | No | No | No |
| o-xylene | Yes | Yes | Yes | No | Yes | No | No |
| o-dichlorobenzene | / | / | / | Yes | / | Yes | Yes |

The penultimate layer to be deposited is the ETL. Poly [(9,9-bis(3'-(N,N-dimethylamino)propyl)-2,7-fluorene)-alt-2,7-(9,9–dioctylfluorene)] (PFN), having been chosen to fulfill this function, shows very good solubility in alcohols such as methanol, ethanol or butanol.[31] To determine the compatibility of the emissive layer with the PFN layer, the various compounds **4a-f** were subjected to these different

alcohols. Thus, thin films of molecules **4a-f** (solutions in *o*-xylene for **4a–e** and *o*-DCB for **4f**) were spin-coated and exposed to the different alcohols. **4f** demonstrated notable solvent resistance, retaining its structural integrity even after washing with 200 µL of MeOH, evidenced by the absence of a reduction in the absorbance spectrum. A 5% and 7% reduction in UV-vis absorption occurred after washing with 200 µL of EtOH and BuOH, respectively (Figure 5b, all graphs in Supplementary Information) which is still acceptable. **4d** also showed very good resistance with MeOH and is a little more soluble in other solvents, whereas the use of **4e** is a little more critical for device manufacture (Figure 5a). **4a-c** were completely washed out. **4f** exhibited optimal solvent resistance characteristics and has the heaviest molecular mass of the series, which is often linked to the solubility.[5] This prompts its selection for testing in OLED devices. Considering *o*-DCB's ability to solubilize PVK completely, the decision was made to fabricate the device without a hole transport layer (HTL).

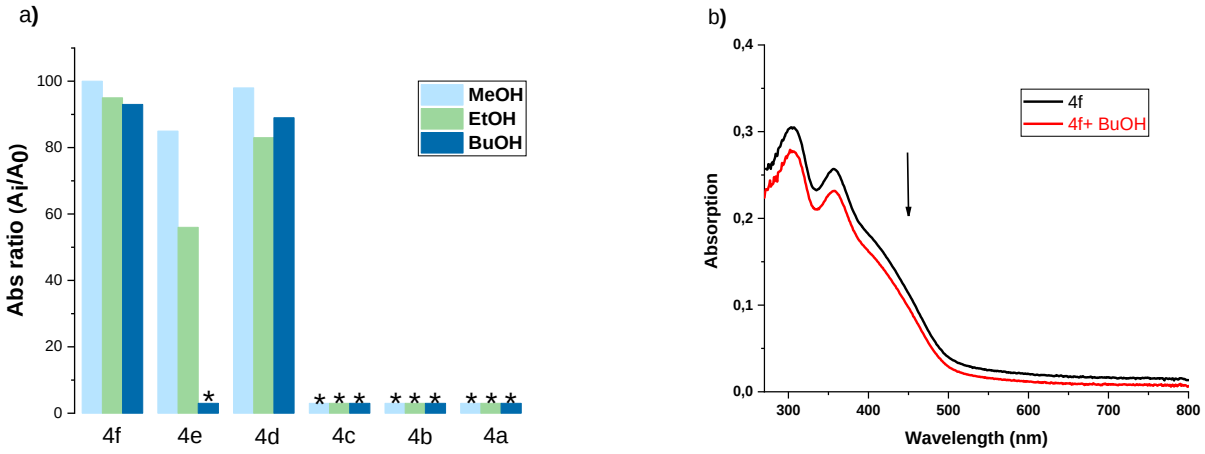


**Figure 5**. a) Solvent resistance of **4a–f** to MeOH, EtOH, and BuOH and b) resistant test illustration for molecule **4f** to BuOH (right). * = (N/A)

Thus, the final configuration for the OLED device, that was retained, is a four-layer structure Glass/ITO (120 nm)/PEDOT:PSS (30 nm)/**4f** (60 nm)/PFN (15 nm)/Ag (100 nm) (see Figure 6).

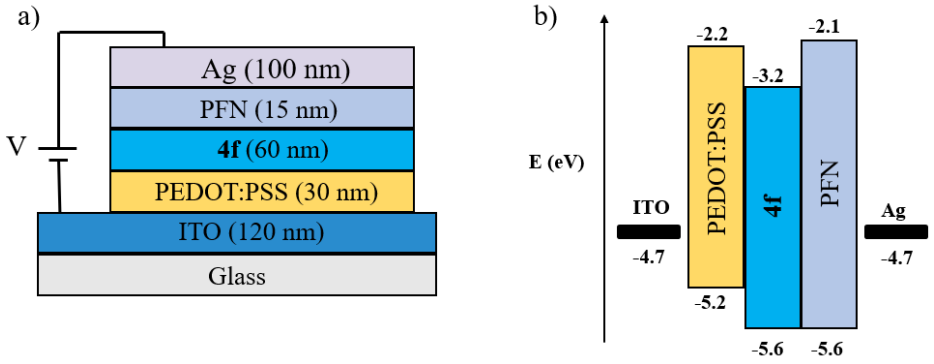

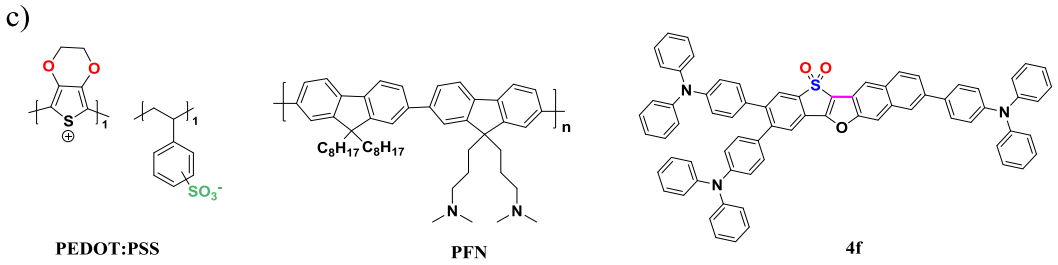


**Figure 6**. a) Device structure. b) Energy diagram of functional materials used in the OLEDs. c) Chemical structures of materials used in this study.

The fabricated device emitted a yellow-green light with CIE coordinates of (0.38, 0.57), as presented in Figure 8. The device exhibited a low turn-on voltage of 3.5 V (see Figure 7), a maximum luminance of 850 cd/m$^2$, a maximum current efficiency of 0.29 cd/A, and a maximum power efficiency of 0.18 lm/W as summarized in Table 4. This is the first report on all solution-processed OLEDs based on BTOBF building blocks. When compared to vacuum-processed OLEDs that have been used,[32] our solution-processed OLED showed comparable performance in terms of turn-on voltage. The typical turn-on voltages of analog devices with BTOBF derivatives as active layers range from 3.6 V to 4.2 V as they use 5 layers vacuum-processed with doped emissive layer with 3,3′-Di(9H-carbazol-9-yl)-1,1′-biphenyl (mCBP) as a host material in comparison with our devices which are 3 layers solution processed in air without any doping and the evaporated cathode. The relatively low turn-on voltage of our device suggests that solution processing could be a promising approach for fabricating high-performance OLEDs with lower operating voltages.

**Table 4**. Device metrics for OLED with **4f**

| Molecule | $V_{turn\text{-}on}$ (V) [a] | $L_{max}$ (cd/m$^2$) [b] | $CE_{max}$ (cd/A) [c] | $PE_{max}$ (lm/W) [d] |
|---|---|---|---|---|
| **4f** | 3.50 | 850 | 0.29 | 0.18 |

[a]$V_{on}$ is the turn-on voltage at 1 cd.m$^2$. [b]Luminance is the maximum luminance of the device. [c]CE, corresponds to current efficiency at maximum luminance. [d] PE corresponds to power efficiency at maximum luminance

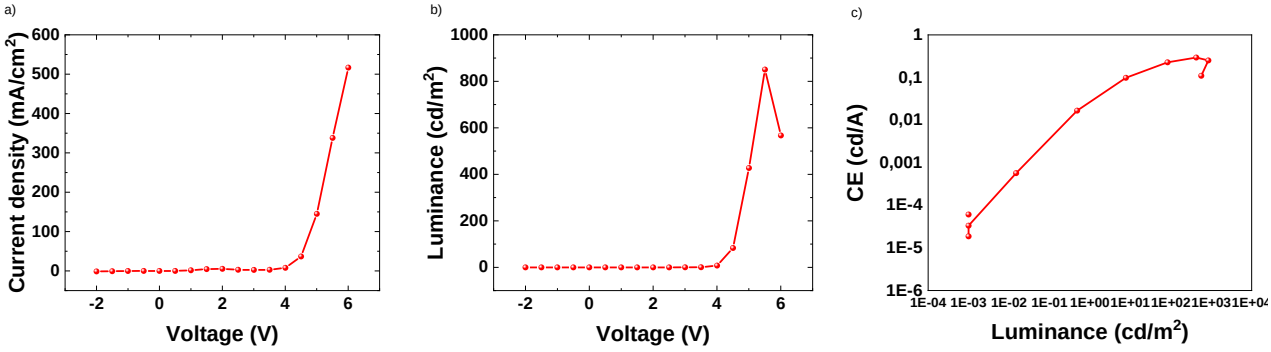


**Figure 7**. a) Current density vs voltage, b) luminance versus voltage, and c) current efficiency versus luminance of the best OLEDs

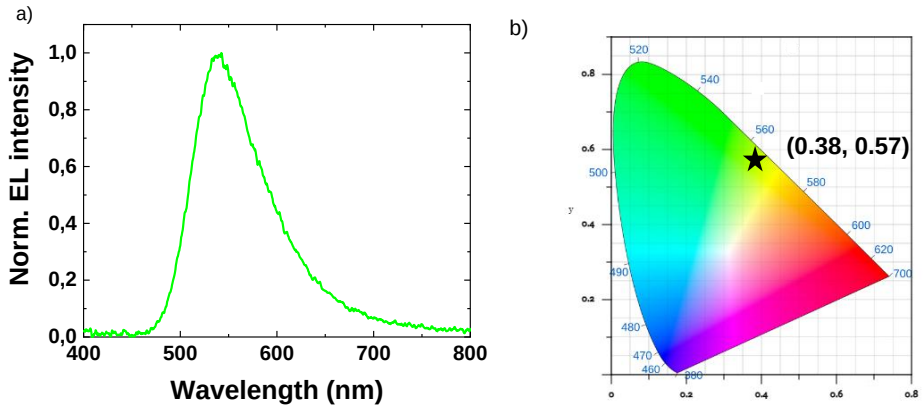


**Figure 8**. a) EL spectrum. b) CIE color coordinates of OLED.

In an exploration of the slot-die coating processability of the small molecule BTOBF, molecule **4f**, known for its good solubility in *o*-DCB, was employed. The chosen materials were applied to ITO coated polyethylene terephthalate (PET) to evaluate their compatibility with flexible substrates. Subsequently, **4f** was slot-die coated in an open-air setting onto a PET/ITO substrate measuring 2 cm in width and 33 cm in length, adopting the same structure as the spin-coated devices, featuring PEDOT: PSS/**4f**/PFN/Ag. Despite successful device activation, an unexpected challenge arose, as the devices initiated but swiftly burned without allowing any data recording. The complexity of this challenge lies in achieving precise morphology control of small-molecule materials. Their extensive surface deposition poses difficulties compared to polymer films, attributed to the low viscosity of their solution, the absence of physical entanglement, higher crystallinity, and the high boiling point of the solvent (*o*-DCB) employed.

## 3- Conclusion

In conclusion, a series of BTOBF-based molecules have been synthesized in high yields with high structure tunability and exhibit dual-state emission with good quantum yields in both states. Photophysical and electrochemical properties were studied and showed the influence of donating and withdrawing groups on modulating absorption and emission properties. For the first time, a solution processed in air organic light emitting diode BTOBF-based was fabricated, with a low turn-on voltage of 3.50 V and good luminance of 850 cd/m$^2$ with just 4 deposited layers. Moreover, we believe that high-performance OLEDs would be realized via the efficient optimization of the chemical structure of BTOBF molecules and device engineering.

## Acknowledgments

This study was financially supported by EUR Lumomat and Angers Loire Métropole (ALM). The stay in Calgary was supported by the Doctoral School ED3MG, EUR Lumomat, and Angers University through the MIR grant.

## Abbreviations

OLED, organic light−emitting diode; PET, polyethylene terephthalate; LUMO, lowest unoccupied molecular orbital; HOMO, highest occupied molecular orbital; HIL, hole injection layer; HTL, hole-transport layer; EML, emitting layer; ETL, electron-transport layer; PEDOT: PSS, poly- (3,4-ethylenedioxythiophene): polystyrene sulfonate. (ITO) indium tin oxide. Ortho-dichlorobenzene (O-DCB).

# References


1. Zou, S.-J.; Shen, Y.; Xie, F.-M.; Chen, J.-D.; Li, Y.-Q.; Tang, J.-X., Recent advances in organic light-emitting diodes: toward smart lighting and displays. *Materials Chemistry Frontiers* **2020,** *4* (3), 788-820.
2. Bui, T.-T.; Goubard, F.; Ibrahim-Ouali, M.; Gigmes, D.; Dumur, F., Recent advances on organic blue thermally activated delayed fluorescence (TADF) emitters for organic light-emitting diodes (OLEDs). *Beilstein Journal of Organic Chemistry* **2018,** *14*, 282-308.
3. Hong, G.; Gan, X.; Leonhardt, C.; Zhang, Z.; Seibert, J.; Busch, J. M.; Bräse, S., A Brief History of OLEDs—Emitter Development and Industry Milestones. *Advanced Materials* **2021,** *33* (9), 2005630.
4. Woo, J. Y.; Park, M.-H.; Jeong, S.-H.; Kim, Y.-H.; Kim, B.; Lee, T.-W.; Han, T.-H., Advances in Solution-Processed OLEDs and their Prospects for Use in Displays. *Advanced Materials* **2023,** *35* (43), 2207454.
5. Aizawa, N.; Pu, Y.-J.; Watanabe, M.; Chiba, T.; Ideta, K.; Toyota, N.; Igarashi, M.; Suzuri, Y.; Sasabe, H.; Kido, J., Solution-processed multilayer small-molecule light-emitting devices with high-efficiency white-light emission. *Nature Communications* **2014,** *5* (1), 5756.
6. Murat, Y.; Petersons, K.; Lanka, D.; Lindvold, L.; Yde, L.; Stensborg, J.; Gerken, M., All solution-processed ITO free flexible organic light-emitting diodes. *Materials Advances* **2020,** *1* (8), 2755-2762.
7. Feng, Z.; Cheng, Z.; Jin, H.; Lu, P., Recent progress of sulphur-containing high-efficiency organic light-emitting diodes (OLEDs). *Journal of Materials Chemistry C* **2022,** *10* (12), 4497-4520.
8. Wei, Q.; Fei, N.; Islam, A.; Lei, T.; Hong, L.; Peng, R.; Fan, X.; Chen, L.; Gao, P.; Ge, Z., Small-Molecule Emitters with High Quantum Efficiency: Mechanisms, Structures, and Applications in OLED Devices. *Advanced Optical Materials* **2018,** *6* (20), 1800512.
9. Hu, L.; Liu, S.; Xie, G.; Yang, W.; Zhang, B., Bis(benzothiophene-S,S-dioxide) fused small molecules realize solution-processible, high-performance and non-doped blue organic light-emitting diodes. *Journal of Materials Chemistry C* **2020,** *8* (3), 1002-1009.
10. Xu, J.; Yang, Y.; Hu, L.; Guo, T.; Zhang, B.; Yang, W.; Cao, Y., Blue light-emitting polymers containing ortho-linking carbazole-based benzothiophene-S, S-dioxide derivative. *Dyes and Pigments* **2017,** *138*, 245-254.
11. Ma, W.; Liu, G.; Zhou, L.; Li, B.; Wang, Y., Benzo[4,5]thieno-S,S-dioxide-[3,2-b]benzofurans: synthesis, properties and application in electroluminescent devices. *Journal of Materials Chemistry C* **2020,** *8* (26), 8796-8803.
12. Meng, H.; Shi, M.; Sun, Y., Thermal excitation delayed blue light material as well as preparation method and application thereof. *CN111440187A* **2020**.
13. Sun, J. W.; Baek, J. Y.; Kim, K.-H.; Moon, C.-K.; Lee, J.-H.; Kwon, S.-K.; Kim, Y.-H.; Kim, J.-J., Thermally Activated Delayed Fluorescence from Azasiline Based Intramolecular Charge-Transfer Emitter (DTPDDA) and a Highly Efficient Blue Light Emitting Diode. *Chemistry of Materials* **2015,** *27* (19), 6675-6681.
14. Pihera, P.; Svoboda, J., Reactivity Studies of [1]Benzothieno[3,2-b][1]benzofuran. *Collect. Czech. Chem. Commun.* **2000,** *65* (1), 58-76.
15. Shi, M.; He, Y.; Sun, Y.; Fang, D.; Miao, J.; Ali, M. U.; Wang, T.; Wang, Y.; Zhang, T.; Meng, H., Bis(diphenylamino)-benzo[4,5]thieno[3,2-b]benzofuran as hole transport material for highly efficient RGB organic light-emitting diodes with low efficiency roll-off and long lifetime. *Organic Electronics* **2020,** *84*, 105793.
16. Wang, J.; He, Y.; Guo, S.; Ali, M. U.; Zhao, C.; Zhu, Y.; Wang, T.; Wang, Y.; Miao, J.; Wei, G.; Meng, H., Multifunctional Benzo[4,5]thieno[3,2-b]benzofuran Derivative with High Mobility and Luminescent Properties. *ACS Applied Materials & Interfaces* **2021,** *13* (10), 12250-12258.
17. Chen, D.; Yuan, D.; Zhang, C.; Wu, H.; Zhang, J.; Li, B.; Zhu, X., Ullmann-Type Intramolecular C–O Reaction Toward Thieno[3,2-b]furan Derivatives with up to Six Fused Rings. *The Journal of Organic Chemistry* **2017,** *82* (20), 10920-10927.

18. Ma, W.; Huang, J.; Li, C.; Jiang, Y.; Li, B.; Qi, T.; Zhu, X., One-pot synthesis and property study on thieno[3,2-b]furan compounds. *RSC Advances* **2019,** *9* (13), 7123-7127.
19. Ai, L.; Ajibola, I. Y.; Li, B., Copper-mediated construction of benzothieno[3,2-b]benzofurans by intramolecular dehydrogenative C–O coupling reaction. *RSC Advances* **2021,** *11* (57), 36305-36309.
20. Saito, K.; Chikkade, P. K.; Kanai, M.; Kuninobu, Y., Palladium-Catalyzed Construction of Heteroatom-Containing π-Conjugated Systems by Intramolecular Oxidative C□H/C□H Coupling Reaction. *Chemistry a European Journal* **2015,** *21* (23), 8365-8368.
21. Kaida, H.; Satoh, T.; Hirano, K.; Miura, M., Synthesis of Thieno[3,2-b]benzofurans by Palladium-catalyzed Intramolecular C–H/C–H Coupling. *Chemistry Letters* **2015,** *44* (8), 1125-1127.
22. Mitsudo, K.; Matsuo, R.; Yonezawa, T.; Inoue, H.; Mandai, H.; Suga, S., Electrochemical Synthesis of Thienoacene Derivatives: Transition-Metal-Free Dehydrogenative C−S Coupling Promoted by a Halogen Mediator. *Angewandte Chemie International Edition* **2020,** *59* (20), 7803-7807.
23. Krishnan R, A.; Babu, S. A.; P. R, N.; Krishnan, J.; John, J., Synthesis of Benzothienobenzofurans via Annulation of Electrophilic Benzothiophenes with Phenols. *Organic Letters* **2021,** *23* (5), 1814-1819.
24. Aitken, R. A.; Bradbury, C. K.; Burns, G.; Morrison, J. J., Tandem Radical Cyclisation in the Flash Vacuum Pyrolysis of 2-Methoxyphenyl and 2-Methylthiophenyl Substituted Phosphorus Ylides. *Synlett* **1995,** *1995* (01), 53-54.
25. Mitsudo, K.; Kobashi, Y.; Nakata, K.; Kurimoto, Y.; Sato, E.; Mandai, H.; Suga, S., Cu-Catalyzed Dehydrogenative C–O Cyclization for the Synthesis of Furan-Fused Thienoacenes. *Organic Letters* **2021,** *23* (11), 4322-4326.
26. Youssef, K.; Allain, M.; Cauchy, T.; Gohier, F., Dimerization reactions with oxidized brominated thiophenes. *New Journal of Chemistry* **2023,** *47* (15), 7375-7380.
27. Instrumentation for Fluorescence Spectroscopy. In *Principles of Fluorescence Spectroscopy*, Lakowicz, J. R., Ed. Springer US: Boston, MA, 2006; pp 27-61.
28. Valeur, B.; Berberan-Santos, M. N., *Molecular fluorescence: principles and applications*. John Wiley & Sons: 2012.
29. Yu, X.; Chang, M.; Chen, W.; Liang, D.; Lu, X.; Zhou, G., Colorless-to-Black Electrochromism from Binary Electrochromes toward Multifunctional Displays. *ACS Applied Materials & Interfaces* **2020,** *12* (35), 39505-39514.
30. Gasonoo, A.; Beaumont, C.; Hoff, A.; Xu, C.; Egberts, P.; Pahlevani, M.; Leclerc, M.; Welch, G. C., Water-Processable Self-Doped Hole-Injection Layer for Large-Area, Air-Processed, Slot-Die-Coated Flexible Organic Light-Emitting Diodes. *Chemistry of Materials* **2023,** *35* (21), 9102-9110.
31. C, A.; Dubey, D. K.; Pahlevani, M.; Welch, G. C., Slot-Die Coating of All Organic/Polymer Layers for Large-Area Flexible OLEDs: Improved Device Performance with Interlayer Modification. *Advanced Materials Technologies* **2021,** *6* (9), 2100264.
32. Ai, L.; Xie, X.; Li, B.; Wang, Y., Pure blue emitters based on benzo[4,5]thieno-S,S-dioxide-[3,2-b]benzofuran with high thermal stability. *Dyes and Pigments* **2023,** *213*, 111153.